Combining End-Effector and Legs Observation for Kinematic Calibration of Parallel Mechanisms

Pierre Renaud, Nicolas Andreff, François Pierrot, Philippe Martinet

Combining end-effector and legs observation for kinematic calibration of parallel mechanisms

Pierre Renaud*[1], Nicolas Andreff*‡, François Pierrot† and Philippe Martinet‡
*LaRAMA
Université Blaise Pascal - IFMA, 63175 Aubière, France
Email: renaud,andreff@ifma.fr
†LIRMM
CNRS - Université Montpellier II, 34090 Montpellier, France
Email: pierrot@lirmm.fr
‡LASMEA
CNRS - Université Blaise Pascal, 63177 Aubière, France
Email: martinet@lasmea.univ-bpclermont.fr

***Abstract*— In this paper, an original approach is proposed for the kinematic calibration of parallel mechanisms. The originality lies in the use of vision to get information on all parts of the mechanism, *i.e.* its end-effector as well as its legs. Metrological redundancy is therefore maximized to improve the calibration efficiency. The approach is implemented for the calibration of the I4 parallel mechanism [1], with the use of the Jacobian matrix. No accurate camera location is needed so that the experimental procedure is easy to achieve. The calibration algorithm is detailed and experimentally demonstrated more efficient than other calibration methods based on legs observation or end-effector observation.**

I. Introduction

Repeatability of parallel mechanisms is considered to be much higher than the repeatability of serial mechanisms [2]. Their accuracy is however limited by the numerous links and passive joints [3]. A kinematic calibration is thus needed. A calibration procedure is based on the minimization of an error function which itself depends on a set of geometrical parameters defining the mechanism. The error function is constituted by gathering redundant information on the mechanism.

Information redundancy may be obtained by measuring the end-effector pose with an exteroceptive sensor. An error function based on the inverse kinematic model [4] is often considered as the most numerically efficient method [5], since an inverse kinematic model can be written in closed-form for most parallel structures, contrary to the direct kinematic model. The main limitation is the necessary end-effector full-pose measurement (position *and* orientation of the end-effector). Only a few measuring devices have been therefore used to conduct parallel structures calibration [4], [6], [7]. The systems are either very expensive, tedious to use or have a low working volume. Vision may constitute an adequate measuring device [8]. In such a case, the pose measurement accuracy is however limited by the measurement volume. The calibration efficiency is therefore restricted by the mechanism workspace. Furthermore, the calibration method sensitivity to the kinematic parameters may become critical when the modelling complexity increases [9].

Besides, the mechanism kinematics are closely linked to the displacements of its legs, *i.e.* the kinematic chains connecting the end-effector to the base. For a Stewart-Gough platform, the Jacobian matrix relating the end-effector velocities to the actuator velocities is for instance defined by the Plücker coordinates of the legs [10]. Information redundancy derived from some measurements on the legs seems therefore an efficient way to achieve the calibration. It may be obtained by installing redundant proprioceptive sensors on some passive joints of the legs [11], [12], [13], [14], as well as kinematic constraints on these elements [15], [16]. Kinematic constraints on the legs however significantly reduces the mechanism workspace, hence the calibration parameter sensitivity. Moreover, the use of additional proprioceptive sensors has to be planned since the mechanism design, and is therefore not applicable to any mechanism.

The legs observation with a camera enables one to get their pose [17], and then to achieve the mechanism kinematic calibration. A calibration method based on the legs observation has been proposed for different classes of parallel mechanisms [9]. In that method, only the legs observation is considered during the calibration. For many mechanisms, the simultaneous observation of the mechanism legs and end-effector can however be achieved. As information redundancy is the basis for the error function design, the calibration efficiency should be logically improved by a simultaneous observation of all the mechanism elements. In this paper, we propose to use vision as a measuring device to get information on the end-effector as well as the legs of an I4 parallel mechanism. The information redundancy, here metrological redundancy, is then maximized while keeping the experimental procedure simple. In particular, the mechanism Jacobian matrix can be used to design the calibration error function.

In the following section the I4 parallel mechanism is described with its modelling. The calibration method is then

[1]P. Renaud was jointly with LaRAMA and LASMEA when doing his PhD on this work, and is now with LIRMM.

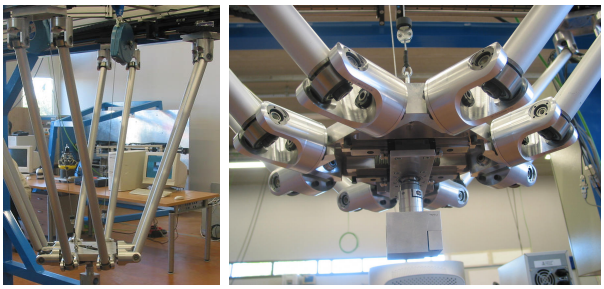

(a) General view (b) Traveling plate view

Fig. 1. The I4 mechanism - General view and traveling plate.

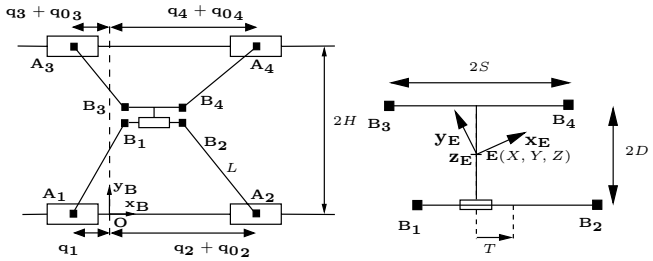

(a) Mechanism (b) Traveling plate

Fig. 2. I4 mechanism geometry.

derived, introducing first the computation of the Jacobian matrix from the image. Experimental results are presented in the fourth section, with comparison to other vision-based kinematic calibration methods, before concluding on the approach and its further developments.

II. Mechanism Modeling

A. Mechanism structure

The I4 mechanism [1] is a four degree-of-freedom mechanism actuated by four linear actuators fixed on the base (figure 1(a)). Four legs link the actuators to a traveling plate which itself supports the end-effector. The end-effector can be translated in three directions, and rotated by the relative displacement of the two plate parts (figure 1(b)), using two rack-and-pinion systems. The workspace volume is approximately equal to $500 \times 400 \times 400\, mm^3$ with a 360° end-effector rotation.

B. Modeling assumptions

The articulated parallelograms that constitute the mechanism legs are modeled by kinematically equivalent single rods of same length linked in $\mathbf{A_i}$, $i \in [1,4]$ and $\mathbf{B_i}$, $i \in [1,4]$ (figure 2(a)).

Because of the manufacturing tolerances, some assumptions achieved during the design of the mechanism are considered valid for the calibration. The efficiency of the design models has moreover been noticed for other parallel mechanism [8]. The actuator axes are considered parallel and coplanar, as well as the point $\mathbf{A_i}$, $i \in [1,4]$, and located on two lines (figure 2(a)). The four single rods are considered identical with a length L.

C. Parameterization

The base frame $R_B(\mathbf{O}, \mathbf{x_B}, \mathbf{y_B}, \mathbf{z_B})$ is defined using as frame origin the joint center $\mathbf{A_1}$ position when the corresponding encoder value is equal to zero (*i.e.* $\mathbf{O} = \mathbf{A_1}|_{q_1=0}$). The four points $\mathbf{A_i}$, $i \in [1,4]$ are located in the $(\mathbf{x_B}, \mathbf{y_B})$ plane and line $\mathbf{A_1A_2}$ is parallel to the $\mathbf{x_B}$ axis.

The end-effector frame $R_E(\mathbf{E}, \mathbf{x_E}, \mathbf{y_E}, \mathbf{z_E})$ is defined with its origin located at the intersection between the revolute joint axis and the plane containing the points $\mathbf{B_i}$, $i \in [1,4]$ (figure 2(b)). The orientation of the vectors $\mathbf{x_E}$ and $\mathbf{y_E}$ is selected to be the same as $\mathbf{x_B}$ and $\mathbf{y_B}$ when the lines $\mathbf{B_1B_3}$ and $\mathbf{B_2B_4}$ are parallel to $\mathbf{y_B}$. The end-effector pose is defined by the position (X, Y, Z) of the end-effector frame origin and its orientation T with respect to the base frame.

Finally, four parameters are needed to define the joints on the base: the distance $2H$ between the two actuator axes and three encoder offsets $\mathbf{q_{0i}}, i \in [2,4]$ so that:

$$(\mathbf{OA_i}) . \mathbf{x_B} = \mathbf{q_i} + \mathbf{q_{0i}} \tag{1}$$

The relative position of the joint centers $\mathbf{B_i}$, $i \in [1,4]$ is defined by the dimensions S and D. Seven parameters finally define the mechanism geometry: $(H, \mathbf{q_{02}}, \mathbf{q_{03}}, \mathbf{q_{04}}, S, D, L)$.

III. Calibration method

A. Two computations of the Jacobian matrix

1) From the kinematic parameters: With the modeling described in the previous section, the Jacobian matrix of the inverse kinematic model with respect to the pose is particularly simple:

$$\mathbf{J_X} = \begin{pmatrix} 1 & \frac{\mathbf{A_1B_1}.\mathbf{y_B}}{\mathbf{A_1B_1}.\mathbf{x_B}} & \frac{\mathbf{A_1B_1}.\mathbf{z_B}}{\mathbf{A_1B_1}.\mathbf{x_B}} & 1 \\ 1 & -\frac{\mathbf{A_1B_1}.\mathbf{y_B}}{\mathbf{A_1B_1}.\mathbf{x_B}} & -\frac{\mathbf{A_1B_1}.\mathbf{z_B}}{\mathbf{A_1B_1}.\mathbf{x_B}} & -1 \\ 1 & \frac{\mathbf{A_3B_3}.\mathbf{y_B}}{\mathbf{A_3B_3}.\mathbf{x_B}} & \frac{\mathbf{A_3B_3}.\mathbf{z_B}}{\mathbf{A_3B_3}.\mathbf{x_B}} & -1 \\ 1 & -\frac{\mathbf{A_3B_3}.\mathbf{y_B}}{\mathbf{A_3B_3}.\mathbf{x_B}} & -\frac{\mathbf{A_3B_3}.\mathbf{z_B}}{\mathbf{A_3B_3}.\mathbf{x_B}} & -1 \end{pmatrix} \tag{2}$$

with $\dot{\mathbf{q}} = (\dot{\mathbf{q}}_1\ \dot{\mathbf{q}}_2\ \dot{\mathbf{q}}_3\ \dot{\mathbf{q}}_4)$, $\dot{\mathbf{X}} = \begin{pmatrix} \dot{\mathbf{X}}\ \dot{\mathbf{Y}}\ \dot{\mathbf{Z}}\ \dot{\mathbf{T}} \end{pmatrix}$ and

$$\dot{\mathbf{q}} = \mathbf{J_X}\dot{\mathbf{X}} \tag{3}$$

The lengths $\|\mathbf{A_iB_i}\|$, $i \in [1,4]$ of the legs are equal. The Jacobian matrix can therefore also be expressed by:

$$\mathbf{J_X} = \begin{pmatrix} 1 & \frac{\mathbf{u_1}.\mathbf{y_B}}{\mathbf{u_1}.\mathbf{x_B}} & \frac{\mathbf{u_1}.\mathbf{z_B}}{\mathbf{u_1}.\mathbf{x_B}} & 1 \\ 1 & -\frac{\mathbf{u_1}.\mathbf{y_B}}{\mathbf{u_1}.\mathbf{x_B}} & -\frac{\mathbf{u_1}.\mathbf{z_B}}{\mathbf{u_1}.\mathbf{x_B}} & -1 \\ 1 & \frac{\mathbf{u_3}.\mathbf{y_B}}{\mathbf{u_3}.\mathbf{x_B}} & \frac{\mathbf{u_3}.\mathbf{z_B}}{\mathbf{u_3}.\mathbf{x_B}} & -1 \\ 1 & -\frac{\mathbf{u_3}.\mathbf{y_B}}{\mathbf{u_3}.\mathbf{x_B}} & -\frac{\mathbf{u_3}.\mathbf{z_B}}{\mathbf{u_3}.\mathbf{x_B}} & -1 \end{pmatrix} \tag{4}$$

with $\mathbf{u_i}$ the leg unit axis vector such that $\mathbf{A_iB_i} = L\mathbf{u_i}$, which can be expressed as a function of the joint values and the kinematic parameters:

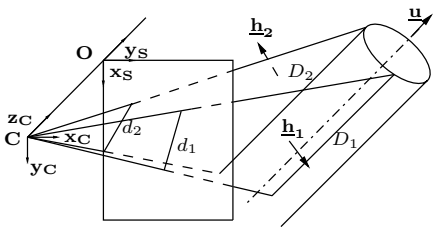

Fig. 3. Cylindrical element observation with a camera.

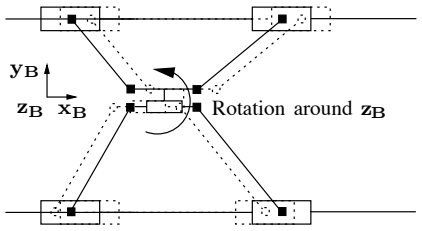

Fig. 4. Determination of the $\mathbf{z_B}$ unit vector in the camera frame.

$$\mathbf{u_1} = \begin{pmatrix} \mathbf{X}-S+\mathbf{T}-\mathbf{q_1} \\ \mathbf{Y}+(H-D) \\ \mathbf{Z} \end{pmatrix} ; \mathbf{u_3} = \begin{pmatrix} \mathbf{X}-S+\mathbf{T}-\mathbf{q_3}-\mathbf{q_{03}} \\ \mathbf{Y}-(H-D) \\ \mathbf{Z} \end{pmatrix}$$

where $(\mathbf{X}, \mathbf{Y}, \mathbf{Z}, \mathbf{T})$ are given from the direct kinematic model [1]:

$$\begin{cases} \mathbf{X}=\frac{\mathbf{q_1}+\mathbf{q_2}+\mathbf{q_3}+\mathbf{q_4}+\mathbf{q_{02}}+\mathbf{q_{03}}+\mathbf{q_{04}}}{4} \\ \mathbf{Y}=\frac{(\mathbf{q_4}-\mathbf{q_3}-2S+\mathbf{q_{04}}-\mathbf{q_{03}})^2-(\mathbf{q_2}-\mathbf{q_1}-2S+\mathbf{q_{02}})^2}{16(H-D)} \\ \mathbf{Z}=-\sqrt{L^2-(H-D)^2-\mathbf{Y}^2-\frac{(\mathbf{q_4}-\mathbf{q_3}-2S+\mathbf{q_{04}}-\mathbf{q_{03}})^2-(\mathbf{q_2}-\mathbf{q_1}-2S+\mathbf{q_{02}})^2}{8}} \\ \mathbf{T}=\frac{\mathbf{q_1}+\mathbf{q_2}-\mathbf{q_3}-\mathbf{q_4}+\mathbf{q_{02}}-\mathbf{q_{03}}-\mathbf{q_{04}}}{4} \end{cases} \quad (5)$$

2) From the image: Let us consider that a camera is observing the legs of the mechanism composed of cylindrical elements, and simultaneously the end-effector equipped with a calibration board. The image formation is supposed to be modeled by the pinhole model [18]. The camera is first calibrated using the calibration board [19] so that optical distortions can be compensated for. It must be noticed that the calibration board geometry is identified simultaneously with the camera. No accurate calibration board is therefore needed, which lowers significantly the measuring system cost and simplify the experimental procedure.

Vision enables us then to compute:

a) From the cylinder observation - A cylinder image is composed of two lines (figure 3), generally intersecting except if the cylinder axis is going through the camera center of projection $\mathbf{C}$. Each cylinder generating line $D_j,\ j \in [1,2]$ corresponding to one line d_j in the image can be defined by its Plücker coordinates [20] $(\mathbf{u}, \mathbf{h_j})$ with $\mathbf{u}$ the cylinder unit axis direction vector and $\mathbf{h_j}$ defined by:

$$\mathbf{h_j} = \mathbf{u} \times \mathbf{CP_j},\ \forall j \in [1,2] \quad (6)$$

where $\mathbf{P_j}$ is an arbitrary point of D_j and $\times$ represents the vector cross product.

One can easily show that $\underline{\mathbf{h_j}} = \mathbf{h_j}/\|\mathbf{h_j}\|$ contains the coefficients of the equation of d_j. The vectors $\underline{\mathbf{h_1}}$, $\underline{\mathbf{h_2}}$ can hence be extracted from the leg image. A cylinder axis direction $\mathbf{u}$ can therefore be computed in the camera frame $R_C(\mathbf{C}, \mathbf{x_C}, \mathbf{y_C}, \mathbf{z_C})$ from (6) by:

$$\mathbf{u} = \frac{\underline{\mathbf{h_1}} \times \underline{\mathbf{h_2}}}{\|\underline{\mathbf{h_1}} \times \underline{\mathbf{h_2}}\|} \quad (7)$$

b) From the calibration board observation - After calibration, a single image of the calibration board enables one to compute the transformation between the frame linked to the camera and the frame linked to the board [19]. The pose of the calibration board can therefore be estimated in the camera frame from its image. It can be noticed that first and fourth matrix columns of the Jacobian matrix (eq. 2) are constant, which expresses that the end-effector displacement along $\mathbf{x_B}$ and rotation around $\mathbf{z_B}$ are not dependent on the mechanism geometry. It is then possible to determine the axes $\mathbf{x_B}$ and $\mathbf{z_B}$ from the calibration board displacement measurement, and from these two vectors to determine the base frame axes in the camera frame.

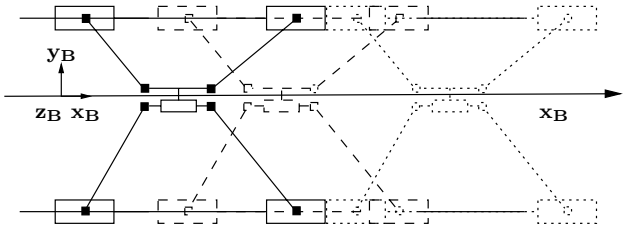

Fig. 5. Determination of the $\mathbf{x_B}$ unit vector in the camera frame.

c) Jacobian matrix estimation - Finally all the elements of the Jacobian matrix can be determined from vision in the camera frame. Due to the scalar product invariance with an Euclidean transformation, an estimation $\tilde{\mathbf{J}}_{\mathbf{X}}$ of the Jacobian matrix can then be computed from the image.

B. Calibration method

In order to be able to compute the Jacobian matrix from the image, the calibration method is composed of two steps:

1) Base frame axes determination in the camera frame: In a first step, two sequential movements of the end-effector enable us to compute the base frame unit vectors:

a) Rotation of the end-effector - The end-effector rotation axis is constant and equal to $\mathbf{z_B}$. Using at least two calibration board positions with different rotations hence enables us to determine the $\mathbf{z_B}$ vector (Figure 4).

b) End-effector translation - Imposing the same displacement to the four linear actuators enables us to move the end-effector in the $\mathbf{x_B}$ direction (figure 5), whatever the kinematic parameters values, as mentioned in the previous section.

From the knowledge of the $\mathbf{x_B}$ and $\mathbf{z_B}$ unit vectors, the vector $\mathbf{y_B}$ can also be computed. It is important to notice that the location of the calibration board with respect to the end-effector does not affect the base frame vectors determination. The experimental procedure is therefore easy to achieve, and no external parameters are introduced in the kinematic

parameter set, contrary to a calibration method based on the inverse kinematic model [8].

2) Kinematic parameters determination: At the end of the first step, all the elements of the Jacobian matrix can be computed in the camera frame for any mechanism pose. The Jacobian matrix can also be computed in the base frame as a function of the kinematic parameters, so that we propose to identify the kinematic parameters by minimizing the error function $F(\xi)$:

$$F(\xi) = \sum_{k=1}^{N} \|\mathbf{J}_{\mathbf{X}k}(\xi) - \tilde{\mathbf{J}_{\mathbf{X}k}}\|_F^2 \quad (8)$$

with $\mathbf{J}_{\mathbf{X}k}(\xi)$ the Jacobian matrix computed as a function of the kinematic parameters (eq. 4) for the k-th pose, $\tilde{\mathbf{J}_{\mathbf{X}k}}$ the corresponding Jacobian matrix computed from the image, N the number of poses considered during the calibration and $\|.\|_F$ the Frobenius matrix norm.

Analytical derivation of the error function shows that a four parameter set $(L, H-D, E-\mathbf{q_{02}}/2, E-(\mathbf{q_{04}}-\mathbf{q_{02}})/2)$ only is identifiable. From the direct kinematic model, one can show that the mechanism accuracy may be then obtained in the $\mathbf{y_B}$ and $\mathbf{z_B}$ directions, and in the $\mathbf{x_B}$ direction and in rotation with a constant error, which is not a major drawback during the use of the mechanism.

IV. Experimental results

In this section, the calibration method efficiency is evaluated experimentally by performing validation tests and by comparison with other vision-based calibration methods, based either on the end-effector observation or the legs observation. These methods are first presented before giving the experimental results.

A. Other calibration methods

1) End-effector observation: The calibration board can be used to achieve the kinematic calibration using an error function based on the inverse kinematic model, as detailed in [8]. The identifiable parameters are then identical to those identified with the proposed method.

2) Legs observation: The calibration method based on the legs observation introduced in [9] is here applied. The parameters are then identified in four steps:

Step 1 The end-effector is displaced while locking sequentially the actuators. For each locked actuator, the position of the corresponding spherical joints that compose the articulated parallelograms can therefore be determined in the camera frame R_C (figure 6). From each couple of spherical joints, one can then compute the joint center $\mathbf{A_i}$, $i \in [1,4]$ in the camera frame and consequently determine the actuator axis $\mathbf{x_B}$ in the camera frame. The position of the points $\mathbf{A_i}$, $i \in [1,4]$ for the actuator encoder zero value can hence be also estimated.

Step 2 The joint centers $\mathbf{A_i}, i \in [1,4]$ are defined in the base frame by four parameters: $(\mathbf{q_{02}}, \mathbf{q_{03}}, \mathbf{q_{04}}, H)$. Due to the scalar product invariance with Euclidean transformation,

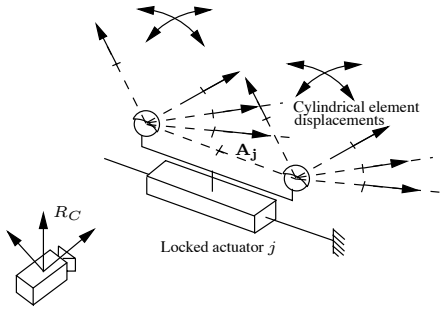

Fig. 6. Identification of the joint centers in the camera frame.

these parameters can be identified by minimizing the error function F':

$$F'(\mathbf{q_{02}}, \mathbf{q_{03}}, \mathbf{q_{04}}, H) = \sum_{(p,q)} [\mathbf{V_p}.\mathbf{V_q}|_{R_C} - \mathbf{V_p}.\mathbf{V_q}|_{R_B}]^2 \quad (9)$$

with the vector set
$\mathbf{V} = (\mathbf{OA_2}|_{\mathbf{q_2}=\mathbf{0}}, \mathbf{OA_3}|_{\mathbf{q_3}=\mathbf{0}}, \mathbf{OA_4}|_{\mathbf{q_4}=\mathbf{0}})$
and

$$\begin{cases} \mathbf{OA_2}|_{\mathbf{q_2}=\mathbf{0}} &= \mathbf{q_{02}}\mathbf{x_B} \\ \mathbf{OA_3}|_{\mathbf{q_3}=\mathbf{0}} &= \mathbf{q_{03}}\mathbf{x_B} + 2H\mathbf{y_B} \\ \mathbf{OA_4}|_{\mathbf{q_4}=\mathbf{0}} &= \mathbf{q_{04}}\mathbf{x_B} + 2H\mathbf{y_B} \end{cases} \quad (10)$$

Six independent equations can be expressed from the elements of $\mathbf{V}$, which ensures the identifiability of the four kinematic parameters.

Step 3 The distances $\|\mathbf{B_1B_2}\|$ and $\|\mathbf{B_3B_4}\|$ are invariant with an end-effector pose modification. Therefore the error function $F_2'(L)$ allows us to determine the length L:

$$F_2'(L) = \sum_{k=1}^{N-1} \Big[\left(\|\mathbf{B_{1,k+1}B_{2,k+1}}\|_{R_C}^2 - \|\mathbf{B_{1,k}B_{2,k}}\|_{R_C}^2 \right)^2 + \left(\|\mathbf{B_{3,k+1}B_{4,k+1}}\|_{R_C}^2 - \|\mathbf{B_{3,k}B_{4,k}}\|_{R_C}^2 \right)^2 \Big] \quad (11)$$

with N the number of poses used for the calibration. Two independent information can be obtained, so that the identifiability of the parameter L is ensured.

Step 4 The distances $\|\mathbf{B_1B_2}\|$ and $\|\mathbf{B_3B_4}\|$ are determined from the previous step and equal to the parameter S, which is therefore immediately estimated. To determine the other dimension D, the relative displacement of the two traveling plate elements has to be taken into account. The distance between $\mathbf{B_1}$ (resp. $\mathbf{B_3}$) and $\mathbf{B_2}$ (resp. $\mathbf{B_4}$) along $\mathbf{y_B}$ is constant and known in the camera frame. The corresponding distance $2D$ is hence also immediately identified.

B. Set-up

The camera is located approximately in the plane $z_B = 0$ at the workspace center in the $\mathbf{y_B}$ and $\mathbf{z_B}$ directions (figure 7), to observe simultaneously the four mechanism legs and the end-effector (figure 8).

The camera has a resolution of 1024×768pixels, 8-bit encoded, with a 3.6mm lens.

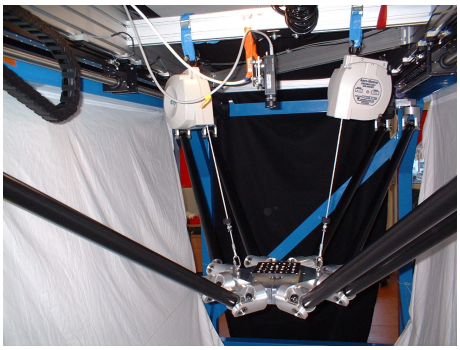

Fig. 7. Experimental set-up.

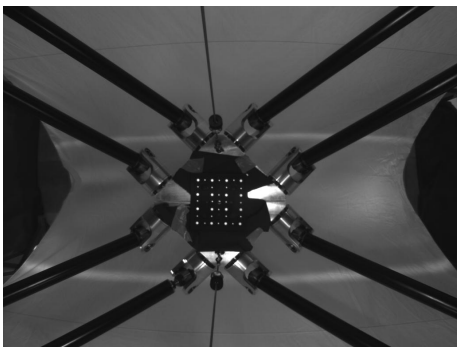

Fig. 8. Legs and calibration board image with the camera.

C. Calibration results

For the proposed method, a 20-pose set is used to determine the base frame unit axes. Another 20-pose set is then used to identify the four kinematic parameters. This latter is also used for the calibration using the end-effector observation. Eventually, for the calibration using only the legs observation, five poses are used to identify each joint center in the first step, and the same 20-pose set used for the other two calibration methods is selected to achieve the second step of the calibration.

The identified parameters with the three calibration methods are indicated in table I. One may notice that the kinematic parameter variation with respect to the *a priori* values and between the different calibration methods are significant: several millimeters for some parameters. In the next section, the influence of such parameter value differences is evaluated through validation tests.

D. Validation tests

1) End-effector displacement analysis: Observation of the calibration board enables us to determine its pose with respect to the camera. The end-effector displacement between two poses can therefore be estimated from these pose measurements. On the other hand, the end-effector displacement can be estimated using the direct kinematic model, the proprioceptive sensor values recorded during the experiment and a kinematic parameter set, either identified or estimated *a priori*. In table II, the mean and root mean squares of the gaps between the vision-based displacement measurements and their estimation are indicated for the parameters identified with the proposed method and the other two algorithms. The gaps are computed for the 20-pose set used for the calibration.

TABLE I

A priori AND IDENTIFIED KINEMATIC PARAMETERS

Parameter	L	$H-D$	$E-\frac{q_{02}}{2}$	$E-\frac{q_{04}-q_{03}}{2}$
a priori	1.001m	0.3464m	-0.6316m	-0.6304m
Legs and end-effector observation				
Identified	0.9949m	0.3297m	-0.6143m	-0.6145m
Legs observation				
Identified	1.0213m	0.3383m	-0.62395m	-0.6240m
End-effector observation				
Identified	1.0068m	0.3475m	-0.6338m	-0.6329m

TABLE II

GAPS BETWEEN VISION-BASED END-EFFECTOR DISPLACEMENT MEASUREMENTS AND THEIR ESTIMATION COMPUTED FROM A KINEMATIC PARAMETER SET.

Parameter set	Mean	Root mean square
a priori	-0.06mm	0.53mm
Identified with the proposed method	-2E-4mm	0.11 mm
Identified from the end-effector observation	3.4E-2mm	0.46 mm
Identified from the legs observation	-3.4E-3mm	0.33 mm

The three calibration methods enable us to lower the gaps between the measured end-effector displacements and their estimation. The most efficient method is however the one proposed in this paper which is based on the use of the information obtained from the end-effector and the legs in the same time. The gap reduction is significant with a RMS reduction by a factor 4.

2) Kinematic constraint: An independent validation test has been also achieved by imposing a kinematic constraint on the end-effector (Figure 9). The end-effector is manually constrained to follow a line materialized by a ruler. The corresponding joint variables are stored. From these joint variable values, poses are computed by means of the direct kinematic model. The physical set-up implies that these poses should lie on a straight line. Hence, the straightness of the line is computed for the kinematic parameter sets (*a priori* and identified) as the root mean square of the distance between the different positions and the line estimated by a least squares criterion.

A $500mm$ line is measured. The straightness measurement repeatability, experimentally evaluated equal to 0.07mm, is in the order of the improvement induced by the calibration (table III). The accuracy improvement can hence not be concluded using this second evaluation criterion. This experiment demonstrates the difficulties that might be encountered while using a kinematic constraint to achieve the calibration of a mechanism with large workspace.

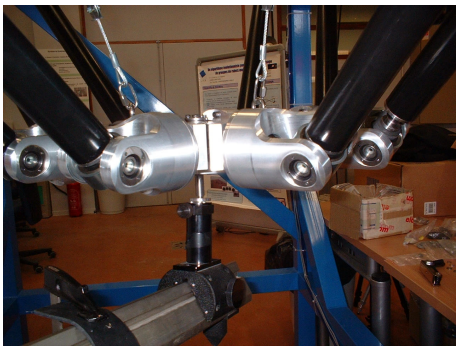

Fig. 9. Experimental set-up for the straightness evaluation.

TABLE III
STRAIGHTNESS EVALUATION WITH THE *a priori* AND IDENTIFIED KINEMATIC PARAMETER SETS.

Parameter set	Straightness
a priori	0.53mm
Identified with the proposed method	0.53mm
Identified from the end-effector observation	0.52mm
Identified from the legs observation	0.50mm

V. CONCLUSION

In this paper, a novel calibration approach has been proposed for parallel mechanisms, based on the use of vision. The simultaneous observation of the mechanism legs and the end-effector enables us to maximize the metrological redundancy, which is intrinsically linked to the method efficiency. Presented for the I4 calibration, the method seems experimentally efficient, with better results than other vision-based calibration methods. The experimental procedure is easy to achieve, and may be performed online.

The presented calibration method has been specifically developed for the I4 mechanism. Further developments will be soon achieved to apply this method to other mechanisms. Vision-based measurements on other leg geometries should be possible, and since the mechanism Jacobian matrix can frequently be derived, the generalization should be achievable. The parameter identifiability with such an approach will need however to be studied thoroughly. Optimization of the mechanism poses for the calibration will also be conducted to improve the procedure efficiency.

ACKNOWLEDGMENT

The authors would like to warmly thank S. Krut for his help during the experiments. This study was jointly funded by CPER Auvergne 2001-2003 program and by the MAX project within the CNRS-ROBEA program.

REFERENCES

[1] S. Krut, O. Company, M. Benoit, H. Ota, and F. Pierrot, "I4: A new parallel mechanism for Scara motions," in *Proceedings of the 2003 International Conference on Robotics and Automation*, Taipei, Taiwan, 2003, pp. 1875–1880, ISBN 0-7803-7399-5.

[2] J.-P. Merlet, *Parallel Robots*. Kluwer Academic Publishers, 2000, ISBN 0-7923-6308-6.

[3] J. Wang and O. Masory, "On the accuracy of a Stewart platform - Part I : The effect of manufacturing tolerances," in *Proceedings of the 1993 IEEE International Conference on Robotics and Automation*, vol. 1, Atlanta, Georgie, 1993, pp. 114–120.

[4] H. Zhuang, J. Yan, and O. Masory, "Calibration of Stewart platforms and other parallel manipulators by minimizing inverse kinematic residuals," *Journal of Robotic Systems*, vol. 15, no. 7, pp. 395–405, 1998.

[5] S. Besnard and W. Khalil, "Identifiable parameters for parallel robots kinematic calibration," in *Proceedings of the 2001 IEEE International Conference on Robotics and Automation*, Seoul, Korea, 2001, pp. 2859–2866.

[6] P. Vischer and R. Clavel, "Kinematic calibration of the parallel delta robot," *Robotica*, vol. 16, pp. 207–218, 1998.

[7] Z. Geng and L. Haynes, "An effective kinematic calibration method for Stewart platform," in *Proceedings of the* 5^{th} *International Symposium on Robotics and Manufacturing*, Hawaï, Hawaï, 1994, pp. 87–92.

[8] P. Renaud, N. Andreff, F. Marquet, and P. Martinet, "Vision-based kinematic calibration of a H4 parallel mechanism," in *Proceedings of the 2003 IEEE International Conference on Robotics and Automation*, Taipei, Taiwan, september 2003, pp. 1191–1196, ISBN 0-7803-7399-5.

[9] P. Renaud, "Apport de la vision pour l'identification géométrique de mécanismes parallèles," Ph.D. dissertation, Université Blaise Pascal, Clermont-Ferrand, september 2003.

[10] J.-P. Merlet, "Parallel manipulators. part 2 - Singular configurations and Grassmann geometry," INRIA, Research report 791, february 1988.

[11] C. Wampler and T. Arai, "Calibration of robots having kinematic closed loops using non-linear least-squares estimation," in *Proceedings of the 1992 IFTOMM World Congress in Mechanism and Machine Science*, Nagoya, Japon, September 1992, pp. 153–158.

[12] H. Zhuang, "Self-calibration of parallel mechanisms with a case study on Stewart platforms," *IEEE Transactions on Robotics and Automation*, vol. 13, no. 3, pp. 387–397, 1997.

[13] D. Daney, "Etalonnage géométrique des robots parallèles," Ph.D. dissertation, Université de Nice - Sophia Antipolis, 2000.

[14] W. Khalil and D. Murareci, "Autonomous calibration of parallel robots," in *Proceedings of the* 5^{th} *IFAC Symposium on Robot Control*, Nantes, France, 1997, pp. 425–428.

[15] W. Khalil and S. Besnard, "Self calibration of Stewart-Gough parallel robots without extra sensors," *IEEE Transactions on Robotics and Automation*, vol. 15, no. 6, pp. 1758–1763, 1999.

[16] D. Daney, "Self calibration of Gough platform using leg mobility constraints," in *Proceedings of the* 10^{th} *world congress on the theory of machine and mechanisms*, Oulu, Finland, 1999, pp. 104–109.

[17] P. Renaud, N. Andreff, G. Gogu, and P. Martinet, "On vision-based kinematic calibration of a stewart-gough platform," in *Proceedings of the* 11^{th} *IFTOMM World congress in mechanism and machine science*, Tianjin, China, april 2004, to appear.

[18] O. Faugeras, *Three-dimensional Computer Vision : A Geometric Viewpoint*. The MIT Press, 1993, ISBN 0-262-06158-9.

[19] J. Lavest and M. Dhome, "Comment calibrer des objectifs très courte focale," in *Actes de Reconnaissance des Formes et Intelligence Artificielle (RFIA2000)*, Paris, France, 2000, pp. 81–90.

[20] H. Pottmann, M. Peternell, and B. Ravani, "Approximation in line space - applications in robot kinematics and surface reconstruction," in *Advances in Robot Kinematics*, Strobl, ISBN 0-7923-5169-X, 1998, pp. 403–412.